Biology of Reproduction, 2024, **111(4)**, 834–844
https://doi.org/10.1093/biolre/ioae106
Advance access publication date 29 June 2024
Research Article

Slit1 inhibits ovarian follicle development and female fertility in mice†

Florine Grudet[1], Emmanuelle Martinot[1], Philippe Godin[1], Michael Bérubé[1], Alain Chédotal[2] and Derek Boerboom[1,*]

[1]Centre de Recherche en Reproduction et Fertilité (CRRF), Département de Biomédecine Vétérinaire, Université de Montréal, Saint-Hyacinthe, QC, Canada
[2]Sorbonne Université, INSERM, CNRS, Institut de la Vision, Paris, France

***Correspondence:** Département de Biomédecine Vétérinaire, Université de Montréal, 3200 Sicotte, Saint-Hyacinthe, QC J2S 2M2, Canada. Tel: 450-773-8521; E-mail: derek.boerboom@umontreal.ca

†**Grant Support:** This work was supported by a project grant from the Natural Sciences and Engineering Research Council of Canada (NSERC) to DB (RGPIN-03745). EM was supported by a postdoctoral fellowship from the Fonds de Recherche du Québec—Santé (FRQS). PG was supported by a doctoral training scholarship from the FRQS. MB was supported by a doctoral training scholarship from the NSERC. The University of Virginia Center for Research in Reproduction Ligand Assay and Analysis Core is supported by the Eunice Kennedy Shriver NICHD/NIH Grant R24HD102061.

Abstract

Previous in vitro studies have suggested that SLIT ligands could play roles in regulating ovarian granulosa cell proliferation and gene expression, as well as luteolysis. However, no in vivo study of *Slit* gene function has been conducted to date. Here, we investigated the potential role of *Slit1* in ovarian biology using a *Slit1*-null mouse model. Female *Slit1*-null mice were found to produce larger litters than their wild-type counterparts due to increased ovulation rates. Increased ovarian weights in *Slit1*-null animals were found to be due to the presence of greater numbers of healthy antral follicles with similar numbers of atretic ones, suggesting both an increased rate of follicle recruitment and a decreased rate of atresia. Consistent with this, treatment of cultured granulosa cells with exogenous SLIT1 induced apoptosis in presence or absence of follicle-stimulating hormone, but had no effect on cell proliferation. Although few alterations in the messenger RNA levels of follicle-stimulating hormone-responsive genes were noted in granulosa cells of *Slit1*-null mice, luteinizing hormone target gene mRNA levels were greatly increased. Finally, increased phospho-AKT levels were found in granulosa cells isolated from *Slit1*-null mice, and SLIT1 pretreatment of cultured granulosa cells inhibited the ability of both follicle-stimulating hormone and luteinizing hormone to increase AKT phosphorylation, suggesting a mechanism whereby SLIT1 could antagonize gonadotropin signaling. These findings therefore represent the first evidence for a physiological role of a SLIT ligand in the ovary, and define *Slit1* as a novel autocrine/paracrine regulator of follicle development.

Summary Sentence

Slit1-null mice are hyperfertile due to enhanced antral follicle survival, ovulation rates, AKT signaling, and gonadotropin-dependent gene expression.

Received: March 12, 2024. **Revised:** June 17, 2024. **Accepted:** June 27, 2024
© The Author(s) 2024. Published by Oxford University Press on behalf of Society for the Study of Reproduction.
This is an Open Access article distributed under the terms of the Creative Commons Attribution Non-Commercial License (https://creativecommons.org/licenses/by-nc/4.0/), which permits non-commercial re-use, distribution, and reproduction in any medium, provided the original work is properly cited.
For commercial re-use, please contact journals.permissions@oup.com

Graphical Abstract

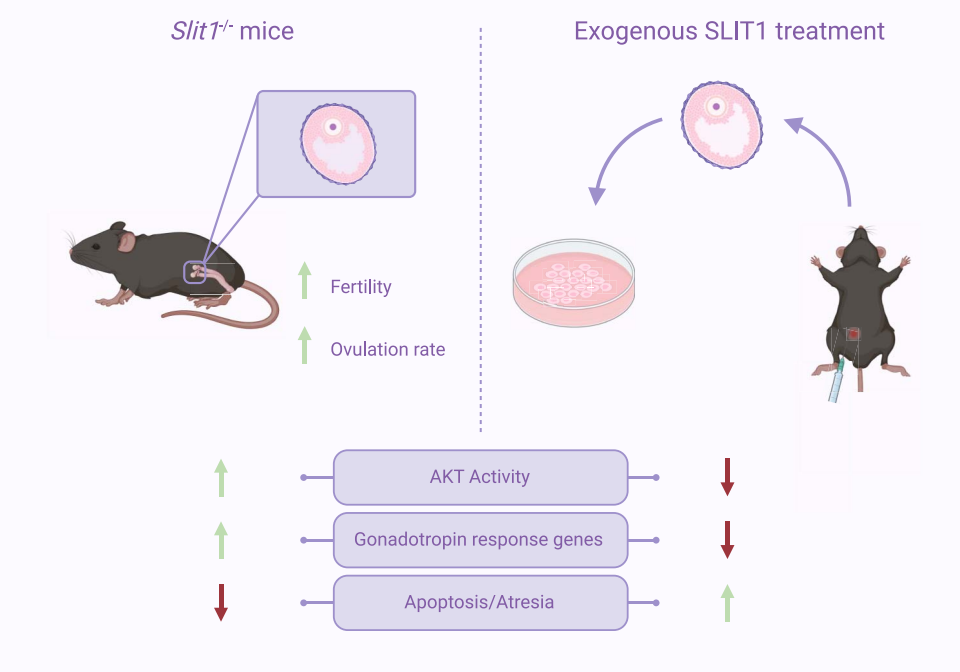

Key words: Slit1, ovary, follicle, atresia, ovulation, progesterone, mouse

Introduction

The ovarian cycle is a tightly regulated process that culminates in release of fertilizable oocytes by the ovary and is essential for the establishment and maintenance of pregnancy. At the endocrine level, it is mainly controlled by the gonadotropins, follicle-stimulating hormone (FSH) and luteinizing hormone (LH), two peptide hormones secreted by the anterior pituitary gland [1]. These act upon follicles at the post-secondary stages of development to regulate their survival and growth, the biosynthesis of steroid hormones, cumulus expansion, ovulation, luteinization, and oocyte maturation [2–6]. Whereas the generation and characterization of *Fshr*- and *Lhcgr*-null mouse models unequivocally proved the essential roles of the gonadotropins in ovarian follicle development [3, 7], it is now clear that a number of additional, intraovarian paracrine and autocrine factors are also required. These factors notably include IGF-1, steroid hormones, prostaglandins, WNTs, fibroblast growth factors, epidermal growth factor-like molecules and several transforming growth factor-β superfamily members. These not only regulate the preantral stages of follicle development (i.e., before gonadotropin responsiveness is acquired) but also subsequently act to coordinate and modulate follicular responses to the gonadotropins [8–20].

Another family of signaling molecules that may play important roles in regulating ovarian follicle development are the SLITs. SLITs are best known for the roles that they play during the development of the central nervous system, as well as for their tumor-suppressive activity in a variety of cell types [21–24]. They act as the ligands for the Roundabout (ROBO) family of single-pass transmembrane receptors. Three *Slit* and four *Robo* genes have been identified, although *Robo3* and *Robo4* are structurally distinct and appears incapable of binding SLIT ligands [23, 25]. Slit/Robo signaling is complex and involves a number of distinct pathways. For instance, in developing neurons, SLITs can signal via Ca^{2+} and small GTPases (RhoA, Rac, Cdc42) to regulate the actin cytoskeletal rearrangements that alter cell adhesion and drive cell migration [23]. More recently, a number of studies from the field of cancer research have shown that SLITs also act by suppressing AKT activity [22, 24] through a mechanism that is not completely understood. Importantly, both FSH and LH signal via AKT [26–28], although it remains unknown if SLIT ligand(s) signal via AKT in follicular cells or if this may modulate gonadotropin signaling in the context of follicle development.

Little is known of the potential roles of Slit/Robo signaling in the ovary. The expression of various *SLIT*s and *ROBO*s has been described in oocytes, granulosa cells, and corpora lutea in women, mice, cows, ewes, and hens [29–34]. *SLIT2/3* and *ROBO2* expression has been shown to increase during luteolysis in women, as does the expression of *Slit2* and *Robo1* in the same context in mice [30, 34]. Pharmacologic inhibition of Slit/Robo signaling was shown to enhance human luteal cell survival in vitro, suggesting a functional role for Slit/Robo in mediating luteolysis [34]. In the hen, genetic manipulation of *SLIT2* and *SLIT3* expression in follicular granulosa cells in vitro showed that they act to inhibit cell proliferation, as well as to reduce the messenger RNA (mRNA) levels of *FSHR* and steroidogenic enzymes, apparently by signaling via ROBO1 and ROBO2 [30, 35, 36] have produced the only in vivo functional analysis of Slit/Robo signaling in the ovary reported thus far. In their study, they examined the reproductive phenotype of mice with a single null allele for both the *Robo1* and *Robo2* genes (i.e. *Robo1*$^{+/-}$; *Robo2*$^{+/-}$). These mice were found to be hyperfertile, apparently due to decreased granulosa cell apoptosis and follicle atresia [30].

In this study, we aimed to determine the role of *Slit1* in mouse ovarian physiology. Using a combination of molecular biology and functional genomics approaches, we found that *Slit1* serves to inhibit follicular AKT activity, gonadotropin-dependent gene expression, granulosa cell and follicle survival, and female fertility.

Material and methods

Animal models, fertility, and ovulation rate assays

Slit1-null mice were as previously described [37] and maintained on a C57BL/6 J genetic background. Mice used in experiments were generated by mating mice that were heterozygous for the null allele, thereby generating *Slit1*-null and wild-type (WT, control) littermates with identical genetic backgrounds. Eight-week-old mice used for follicle counting, hormone measurements and immunohistochemistry were sacrificed during diestrus, as determined by vaginal cytology [38]. Fertility was assessed by mating 8-week-old *Slit1*-null ($n = 12$) and control ($n = 10$) females with WT males for a period of 6 months and counting numbers of litters and pups (at birth) produced. Males were removed after 6 months and the females monitored for 3 weeks for the production of a final litter. Ovulation rates were determined by housing 8-week-old *Slit1*-null ($n = 6$) and control ($n = 6$) females with WT males and monitoring daily for the presence of a copulatory plug. Females were sacrificed on the morning that the plug was observed, the oviducts isolated and placed in saline solution in a Petri dish, and the ovulated cumulus–oocyte complexes (COCs) released by tearing the ampullae of the oviducts with forceps. Retrograde flushing with saline was also done to expel any remaining COCs. The experiment was also performed using immature (22- to 25-day-old) *Slit1*-null ($n = 5$) and WT ($n = 6$) female mice stimulated with 5 IU (IP) of equine chorionic gonadotropin (eCG; Folligon, Merck) followed 48 h later by an ovulatory dose (5 IU, IP) of human chorionic gonadotropin (hCG; Chorulon, Merck). The mice were sacrificed 24 h afterward and the COCs isolated and counted as described above. All animal procedures were approved by the Comité d'éthique de l'utilisation des animaux (CÉUA—Institutional Animal Care and Use Committee) of the Faculté de médecine vétérinaire of the Université de Montréal and conformed to the International Guiding Principles for Biomedical Research Involving Animals.

Follicle counting

Antral follicle counting and atresia scoring was done as previously described [38]. Briefly, left ovaries from 8-week-old Slit1-null ($n = 8$) and WT ($n = 9$) mice were fixed in 10% formalin prior to paraffin embedding. Ovaries were then serially sectioned at a thickness of 6 μm, and every fifth section was stained with hematoxylin and eosin. All antral follicles (corresponding to Pedersen classes 6–8 [39]) with a visible oocyte nucleus were counted and scored as healthy or atretic. The primary criteria of atresia scoring were (1) presence and degree of pyknosis (condensed granulosa cells or cells with condensed nuclei), (2) presence and degree of loss of granulosa cell attachment to oocytes or loss of cumulus cells, and (3) presence of polymorphonuclear neutrophils. Secondary criteria were granulosa cell vacuolation, sparse or missing granulosa cells, and integrity of the basement membrane.

Granulosa cell isolation and culture

Granulosa cells were isolated from the ovaries of immature, eCG- or eCG/hCG-treated (see above) *Slit1*-null and WT mice using the needle puncture technique [40], followed by filtration using 40 μM cell strainers (Progene 71-229481-ULT, Ultident, St-Laurent, QC, Canada) to remove debris and COCs. Recovered cells were then analyzed by Western blotting or RT-qPCR (see below) or seeded onto 96-well plates (ThermoFisher Scientific) (cells from 0.5 ovary per well) in MEM 1X (ThermoFisher Scientific) supplemented with 0.25 mM sodium pyruvate (ThermoFisher Scientific), 3 mM L-glutamine (Wisent Inc.), penicillin–streptomycin (Wisent Inc.), and 1% fetal bovine serum (FBS; Wisent Inc.) and incubated (5% CO_2/95% air) for 3 h at 37°C to attach. Cells were then serum-starved for 2 h before treatment (or not) with 50 ng/ml human recombinant LH or FSH (National Hormone & Peptide Program) or PBS (control). Recombinant mouse SLIT1 (10 μg/ml) (5199-SL-050, R&D systems) was added 1 h prior to gonadotropin treatment in certain groups. Slightly different culture and treatment conditions were used for the TUNEL and flow cytometry assays, as described below.

Immunohistochemistry

Ovaries obtained from adult or immature mice 48 h after eCG were fixed in 10% formalin and paraffin-embedded. Following sectioning (3 μm), deparaffinization, rehydration, and sodium citrate heat-mediated antigen retrieval, sections were incubated with anti-SLIT1 (Santa Cruz, sc-376,756, 1:250) or Cleaved Caspase 3 (Cell Signaling, 9661, 1:200) primary antibody overnight. Detection was performed using the Vectastain Elite ABC Horseradish peroxidase (HRP) Kit followed by the DAB Peroxidase (HRP) Substrate Kit according to the manufacturer's instructions (Vector Laboratories). Slides were counterstained with hematoxylin prior to mounting.

Western blotting

Proteins were extracted from freshly isolated or cultured granulosa cells (GCs) by lysis in sodium dodecyl sulphate (SDS) loading buffer containing 5% β-mercaptoethanol (BioShop). Samples were resolved on 4–10% precast polyacrylamide gels (Biorad, #5678095) and transferred to low-autofluorescence PVDF membranes (Biorad, #1704275). Membranes were blocked with 5% non-fat dry milk in Tris-buffered saline supplemented with 0.1% Tween 20 (BioShop) (TBST) and probed with antibodies raised against Phospho-AKT(S473) (Cell Signaling, 4060, 1:1000), AKT (Cell Signaling, 4691, 1:1000), or Cleaved Caspase 3 (Cell Signaling, 9661, 1:500) overnight at 4°C in TBST supplemented with 5% BSA (Bioshop). Membranes were then probed with anti-rabbit IgG HRP Conjugate (Promega) diluted in 5% non-fat powdered milk for 1 h at room temperature. The antibody against ACTB (β-actin, loading control, sc-47778) was diluted 1:10 000 in 5% non-fat powdered milk and incubated for 1 h at room temperature. Luminescent signal was generated using Immobilon Western Chemiluminescent HRP substrate (MilliporeSigma). Images were captured with ChemiDoc MP Imaging System (Bio-Rad) and signals quantified using Image Lab Software v.5.0 (Bio-Rad).

Real-time polymerase chain reaction analyses

Total RNA from granulosa cells was extracted, quantified, and reverse-transcribed as previously described [41].

Polymerase chain reactions consisted of 2.3 μl of water, 6 pmol of each forward and reverse gene-specific primer, 7.5 μl of Advanced qPCR mastermix with Supergreen Lo-ROX (Wisent Inc.), and 4 μl of cDNA (diluted 10-fold from the RT reactions). Specific primer sequences are listed in Supplementary Table 1. Real-time PCR reactions were run using a CFX96 Touch Real-Time PCR Detection System (Bio-Rad). The thermal cycling program was the same in all cases, and as previously described [41]. Messenger RNA levels were determined using CFX ManagerTM Software 3.0 (Bio-Rad), with the mathematical model according to Pfaffl [42] and using *Rpl19* as the housekeeping gene.

Flow cytometry analyses

Granulosa cells were seeded onto 24-well culture plates (10^6 cells per well) and cultured in Dulbecco's Modified Eagle Medium (DMEM)/F12 (Wisent, 319-085-CL) medium supplemented with 10% FBS and penicillin/streptomycin and incubated for 24 h (37°C; 5% CO_2). Following 24 h of treatment with SLIT1 (10 μg/ml) or vehicle (PBS) ($n = 4$ wells/treatment) cells were trypsinized, centrifuged (1200 *g* for 10 min), and fixed in 70% ethanol overnight at 4°C. Cells were washed and stained with RNase A (ThermoFisher Scientific, EN0531) and PI (Merck, 537060-5ML) solution and incubated at 37°C for 30 min in the dark. The proportion of cells in each phase of the cycle was then assessed (30 000 cells/analysis) using a BD Accuri C6 Flow Cytometer (BD Biosciences) and FlowJo 10.6.2 software (BD Biosciences).

TUNEL assays

Granulosa cells were seeded in 8-well chamber slides (2×10^6 per well) (Thermo Scientific, #154941). Cells were cultured in DMEM supplemented with 1% FBS for 3 h prior to treatment with SLIT1 or vehicle (PBS) for 1 h, followed by and FSH or vehicle (PBS) for 4 h. The medium was removed, and cells were labeled using the In Situ Cell Death Detection Kit, TMR red (Roche, #12156792910) according to the manufacturer's instructions. The percentage of dead cells was quantified using ImageJ 1.53a software [43] as previously described [44] on monochrome images ($n = 16$/treatment).

Hormonal assays

Blood samples were collected by cardiac puncture prior to euthanasia and allowed to clot at room temperature for 90 min. Following centrifugation at 2000 *g* for 15 min at room temperature, serum samples were transferred to polypropylene tubes and stored at −80°C until analyzed. Serum estradiol levels were determined by ELISA, whereas LH and FSH levels were determined by radioimmunoassay (RIA). Progesterone levels in serum and in spent culture media were determined by RIA. All assays were performed by the Ligand Assay and Analysis Core Laboratory of the University of Virginia (Charlottesville, VA).

Statistical analyses

Normality was assessed using the Shapiro–Wilk test. When data followed a normal distribution, the Student *t*-test was used whenever two groups were to be compared. For analyses involving more than two groups, ANOVA (one-way or two-way) was conducted, followed by the Bonferroni multiple comparison test. In cases where the data deviated from a normal distribution, a Mann–Whitney test was used whenever two groups were to be compared. In cases involving more than two groups, the Kruskal–Wallis test followed by the Dunn multiple comparison test was performed. Fertility data were analyzed using the chi-square test. Statistical analyses were done using GraphPad Prism software version 10.1.0 (GraphPad Software) and Rstudio (R version 4.2.1). Data are presented as means ± SEM. $P \leq 0.05$ was considered statistically significant.

Results

To identify *Slit* gene(s) that may have biological roles in ovarian granulosa cells, an initial screening was conducted in which primary cultures of mouse granulosa cells were pretreated with recombinant SLIT ligands, followed or not by addition of gonadotropin. Cells were then monitored for changes in the activity of several signal transduction pathways and the mRNA levels of key ovarian genes. From these initial experiments, SLIT1 was found to suppress the phosphorylation of AKT (Figure 1A and B), as well as to antagonize the LH-induced increase in the mRNA levels of *Ereg* and *Star*. The latter effects were found to be dose-dependent (Figure 1C) as well as time-dependent (Figure 1D), reaching maximal effect 1 h post-LH treatment. Decreases in StAR mRNA levels were also accompanied by decreased levels of progesterone in spent culture media (Figure 1E). In vivo ovarian *Slit1* expression was then studied by immunohistochemistry and RT-qPCR on a time course using the gonadotropin-primed immature mouse model. Results showed high and invariant levels of *Slit1* mRNA throughout antral follicle development (i.e., 0–48 h post-eCG) and throughout the hCG-induced ovulatory process (Supplementary Figure 1A). Immunohistochemistry analyses showed abundant *Slit1* expression in follicles from the secondary stage through ovulation, and apparently localizing exclusively to the granulosa cells, as well as to luteal cells in adult mice (Supplementary Figure 1B). On the basis of these findings, *Slit1* was selected for subsequent in vivo functional analyses.

To elucidate the roles of *Slit1* in the ovary, female *Slit1*-null mice [37] were first housed with WT male mice and their fertility assessed by counting numbers of litters and pups produced over a period of 6 months. Although *Slit1*-null females produced numbers of litters comparable to their (control) WT littermates, their litter sizes were significantly larger (≈0.8 pup/litter, Table 1). To determine if this increased fertility was due to an increased ovulation rate, cumulus–oocyte complexes were retrieved from the oviducts of adult *Slit1*-null mice following natural mating, as well as from immature mice following eCG/hCG superovulation. In both cases, *Slit1*-null animals produced significantly higher numbers of ovulated COCs than their WT controls (Table 2). Analyses of ovarian weights at 2, 6, and 9 months of age showed ovaries from Slit1-null mice to be ≈25–50% heavier than those of their WT counterparts (Supplementary Figure 2), and initial histologic analyses suggested that this could be due to an increased abundance of large follicles (Supplementary Figure 3). A follicle-counting experiment using serial sectioning was therefore conducted to quantify any potential changes in follicular development dynamics. This revealed larger numbers of total and healthy antral follicles in the ovaries of 8-week-old *Slit1*-null mice compared to their WT littermates, whereas numbers of antral follicles undergoing atresia were comparable between groups (Table 3, Supplementary Figure 3).

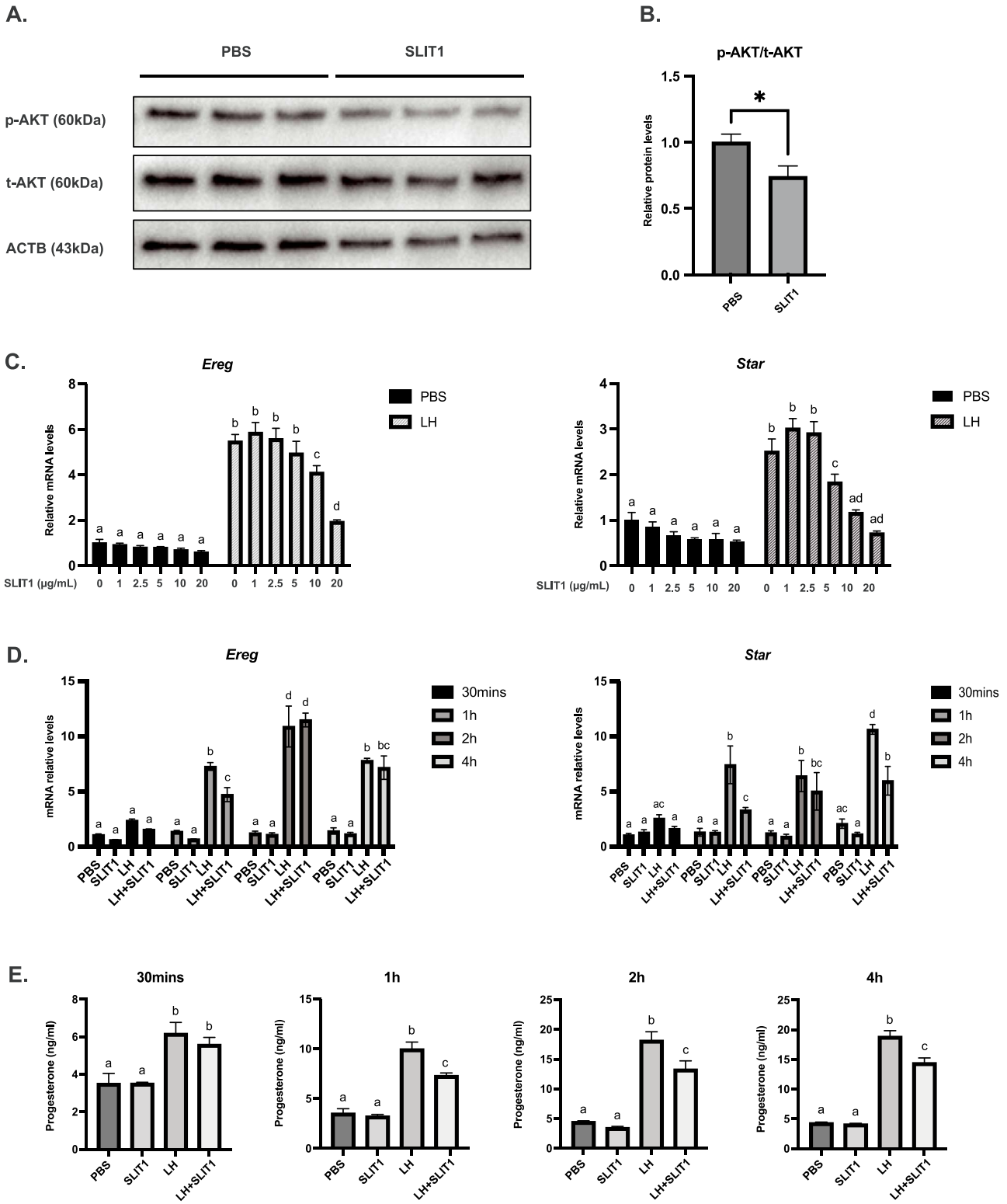

Figure 1. Bioactivity of recombinant SLIT1 in primary granulosa cell cultures. (A) Immunoblotting analyses of total AKT (t-AKT) and phospho-AKT (p-AKT) levels in granulosa cells treated or not with SLIT1, with ACTB (β-actin) serving as a loading control. (B) Densitometric analysis of the immunoblotting experiment depicted in A ($n = 6$/group). (C) Dose–response analysis of *Ereg* and *Star* mRNA levels in granulosa cells pretreated with graded doses of SLIT1, followed (or not) by LH treatment ($n = 4$/group). (D) Time course analysis of *Ereg* and *Star* mRNA levels in granulosa cells pretreated (or not) with SLIT1 (10 μg/ml), followed (or not) by LH treatment for the indicated times ($n = 4$/group). (E) Progesterone levels in spent culture media from the experiment shown in (D). Columns = means, error bars = SEM, statistically significant differences between groups ($P < 0.05$) are indicated with an asterisk (*) or with letters; columns lacking a common letter being significantly different from one another.

Table 1. Fertility trial

	WT	*Slit1* $^{-/-}$
n	10	12
No. of litters	5.6 ± 0.22	6.08 ± 0.14
Total pups	35.1 ± 2.59	43.08 ± 1.90*
Litter size	6.24 ± 0.31	7.07 ± 0.25*

*Significantly different from control, $P < 0.05$.

Table 2. Ovulation rates

	WT	*Slit1* $^{-/-}$
Superovulation	26.3 ± 3.77	43.2 ± 5.63*
Natural mating	9.0 ± 0.63	12.7 ± 0.56**

*Significantly different from control, $P < 0.05$. **Significantly different from control, $P < 0.01$.

Table 3. Antral follicle counts

	WT	*Slit1*$^{-/-}$
Healthy follicles	9.78 ± 1.14	14.25 ± 1.49*
Atretic follicles	1.44 ± 0.41	2.0 ± 0.44
Total	11.22 ± 1.43	17.0 ± 2.18*

*Significantly different from control, $P < 0.05$.

Table 4. Cell cycle assay

	PBS	SLIT1
G1 (%)	82.94 ± 3.41	83.32 ± 1.90
S (%)	4.14 ± 2.73	5.89 ± 2.34
G2/M (%)	12.23 ± 2.20	10.26 ± 1.90

These findings suggested both an increased rate of follicle recruitment and a decreased rate of atresia occurring in the ovaries of *Slit1*-null mice.

To evaluate the effects of SLIT1 on granulosa cell proliferation, granulosa cells from WT mice were placed in culture and treated (or not) with SLIT1 and subjected to propidium iodide staining/Fluorescence-activated cell sorting (FACS) assays. SLIT1 treatment had no measurable effect on the proportion of granulosa cells in any phase of the cell cycle (Table 4). To determine the effects of SLIT1 on granulosa cell apoptosis, similar cultures were treated with SLIT1 and/or FSH, and analyzed by TUNEL. These assays showed that SLIT1 induces apoptosis in vitro, either in presence of absence of FSH (Figure 2A and B). Comparable results were obtained when apoptosis was detected by measurement of cleaved Caspase-3 expression by western blotting (Figure 2C and D). Together with the in vivo findings, these results suggest that loss of *Slit1* enhanced granulosa cell and follicle survival, leading to larger numbers of follicles being available to ovulate, with resultant increased ovulation rates and enhanced fertility.

To determine the molecular basis for the changes in ovarian physiology in *Slit1*-null mice, mRNA levels of key gonadotropin response genes were determined by RT-qPCR in granulosa cells isolated from the ovaries of immature mice following eCG treatment for 48 h, as well as from additional groups that received a subsequent hCG treatment for 4 or 12 h. Results showed few changes in the mRNA levels of FSH-responsive genes at 48 h post-eCG relative to controls, although a significant decrease in *Fshr* mRNA levels was noted in the *Slit1*-null group (Figure 3A). Consistent with the lack of changes in the expression of FSH-regulated steroidogenesis-related genes (i.e., *Nr5a2*, *Cyp19a1*), serum estradiol levels were also comparable between groups (Supplementary Table 2).

Unlike what was observed for FSH-responsive genes at 48 h post-eCG, granulosa cells from *Slit1*-null mice had increased mRNA levels of many LH-responsive genes following hCG treatment, particularly at 12 h (Figure 3B and C). These included groups of genes involved in ovulation/luteinization (i.e., *Pgr*, *Vegfa*, *Klf4*), extracellular matrix remodeling, and cumulus expansion (i.e., *Adamts1*, *Ptx3*, *Has2*), as well as luteal cell steroidogenesis (i.e., *Nr5a2*, *Star*, *Cyp11a1*, *Hsd3b2*). Although the latter finding complemented the suppression of LH-induced *Star* mRNA levels and progesterone secretion that we had observed in granulosa cells in response to SLIT1 *in vitro* (Figure 1), circulating progesterone levels were not abnormally increased following hCG treatment in immature *Slit1*-null mice and were also comparable to controls in adult mice (Supplementary Table 2). This unexpected lack of change was not due to a compensatory effect higher in the hypothalamo-pituitary-gonadal (HPG) axis, as circulating FSH and LH levels were also found to be comparable between groups (Supplementary Table 2). Together, these findings suggest that *Slit1* acts to antagonize the regulation by the gonadotropins (particularly LH) of at least a subset of their target genes.

To begin delineating the signaling mechanism whereby *Slit1* may regulate gonadotropin target gene expression and promote apoptosis in granulosa cells, we examined the effect of exogenous SLIT1 on gonadotropin-regulated AKT phosphorylation levels in cultured granulosa cells from WT mice. Results showed that SLIT1 pretreatment inhibited the ability of both FSH and LH to induce AKT activity (Figure 4A–D). Similar results were obtained when this experiment was conducted using cells isolated from *Slit1*-null mice. Importantly however, intrinsic levels of AKT phosphorylation were found to be significantly higher in granulosa cells from *Slit1*-null mice relative to controls (Figure 4A–D), indicating that *Slit1* serves to suppress AKT signaling in granulosa cells in vivo.

Discussion

A handful of previous studies have employed pharmacologic and genetic approaches to manipulate SLIT expression or signaling in ovarian follicular granulosa cells, resulting in altered proliferation, apoptosis and gene expression [30, 34–36, 45]. These have suggested potential physiological roles for Slit/Robo signaling in mediating processes such as follicle selection and growth, as well as luteolysis. However, no study to date has examined the physiological roles of SLIT ligands in the ovary in vivo. Here, using a *Slit1*-null mouse model and complementary in vitro assays using cultured granulosa cells treated with recombinant SLIT1, we show that *Slit1* serves as a positive regulator of granulosa cell apoptosis and follicular atresia. In absence of *Slit1*, a decreased rate of follicle atresia was observed, with accompanying increased numbers of healthy follicles, increased ovulation rates, and hyperfertility. Conversely, SLIT1 treatment induced granulosa cell apoptosis in vitro. These findings define *Slit1* as a novel regulator of follicle development and, together with a previous

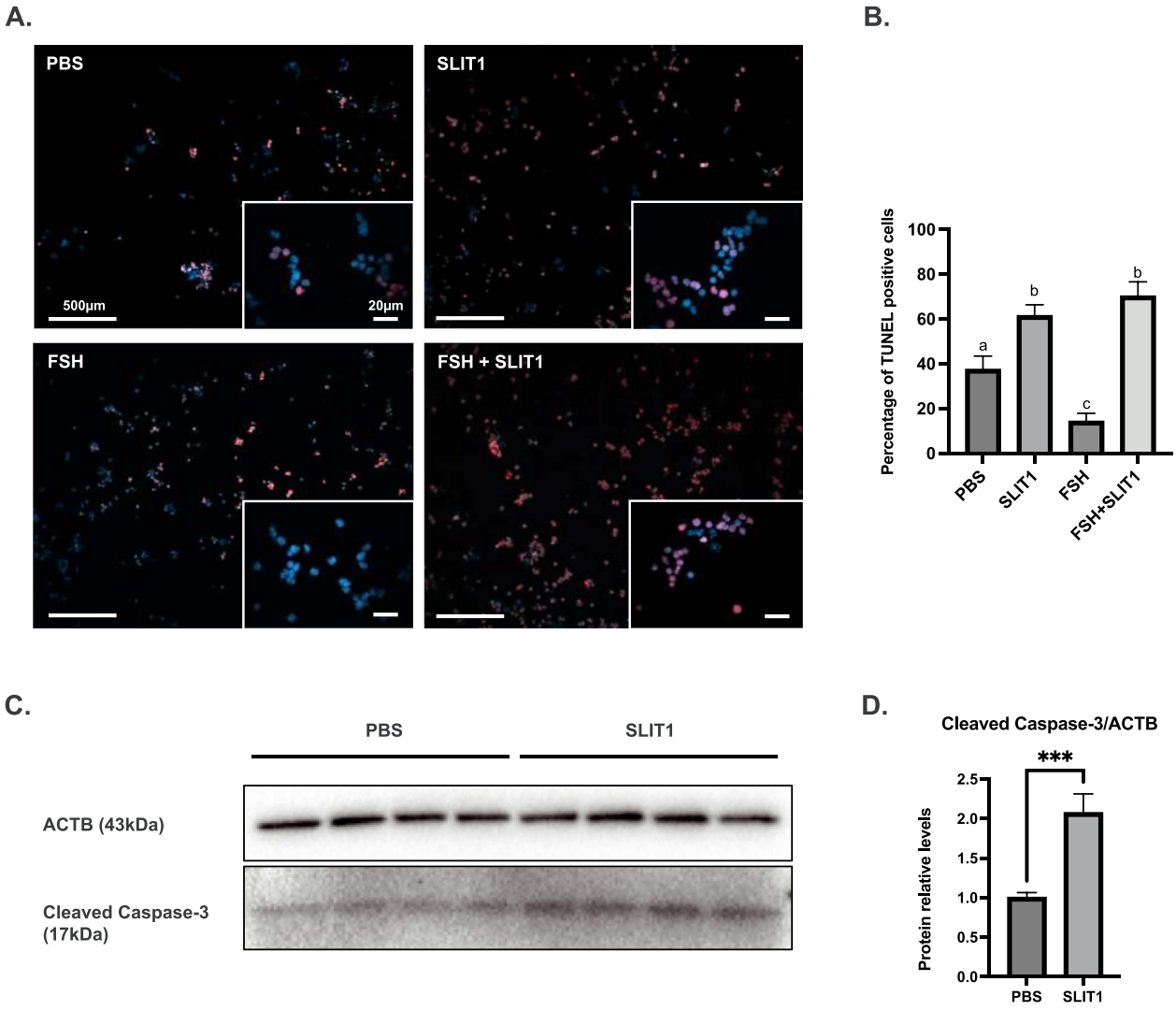

Figure 2. Recombinant SLIT1 induces apoptosis in primary granulosa cell cultures. (A) Representative photomicrographs (bar = 500 μM) of TUNEL analyses of granulosa cells pretreated (or not) with SLIT1 (10 μg/ml), followed (or) not by FSH treatment. Insets: high-magnification images (bar = 20 μM). Red = TUNEL signal, blue = DAPI counterstain. (B) Quantitative analysis of the experiment depicted in (A). (C) Immunoblotting analyses of cleaved Caspase-3 expression in granulosa cells treated or not with SLIT1 (10 μg/ml), with ACTB (β-actin) serving as a loading control. (D) Densitometric analysis of the immunoblotting experiment depicted in (C) ($n = 6$/group). Columns = means, error bars = SEM, statistically significant differences between groups ($P < 0.001$) are indicated with asterisks (***) or with letters; columns lacking a common letter being significantly different ($P < 0.05$) from one another.

study of the ovarian functions of *Robo1* and *Robo2* [30], indicate that Slit/Robo signaling serves as an intra-ovarian mechanism that limits female fertility by inhibiting follicle survival.

Further investigation will be required to fully elucidate the mechanisms whereby *Slit1* exerts its effects in granulosa cells. Our initial findings show that it inhibits AKT activity, as has been shown in other cell types, notably in the context of tumor suppression [46, 47]. Both FSH and LH signal via AKT [26, 27, 48, 49], and indeed our data indicate that *Slit1* can counteract their ability to increase AKT activity. FSH is well-known to act as a follicle survival factor, notably by inhibiting autophagy and apoptosis through activation of AKT and mTOR [50]. It is therefore tempting to speculate that *Slit1* promotes follicular atresia by antagonizing an FSH-regulated AKT survival signal. However, our data suggest that *Slit1* has little or no effect on other key physiologic effects of FSH, such as promoting cell proliferation and estradiol secretion, nor does it appear to have much effect on the expression of FSH target genes. The latter finding was particularly surprising given that FSH regulates a large proportion of its target genes by signaling via AKT and FOXO1 [51]. One potential explanation for this is the decreased expression of *Fshr* that we observed in the granulosa cells of *Slit1*-null mice, which could represent a compensatory response that decreases FSH responsiveness, thereby maintaining relatively normal proliferation, steroidogenesis, and target gene expression despite increased AKT activity. The mechanism whereby *Slit1* promotes granulosa cell apoptosis would therefore seem to be either independent of its AKT-regulatory effects, or it involves the suppression of AKT signaling in a manner that somehow does not interfere with other aspects of FSH action.

Increased ovulatory efficiency in *Slit1*-null mice appeared to be the result of increased numbers of healthy antral follicles present in the ovary and hence larger cohorts of follicles available to ovulate with every cycle. However, we cannot exclude that an enhanced response to LH also contributed to this

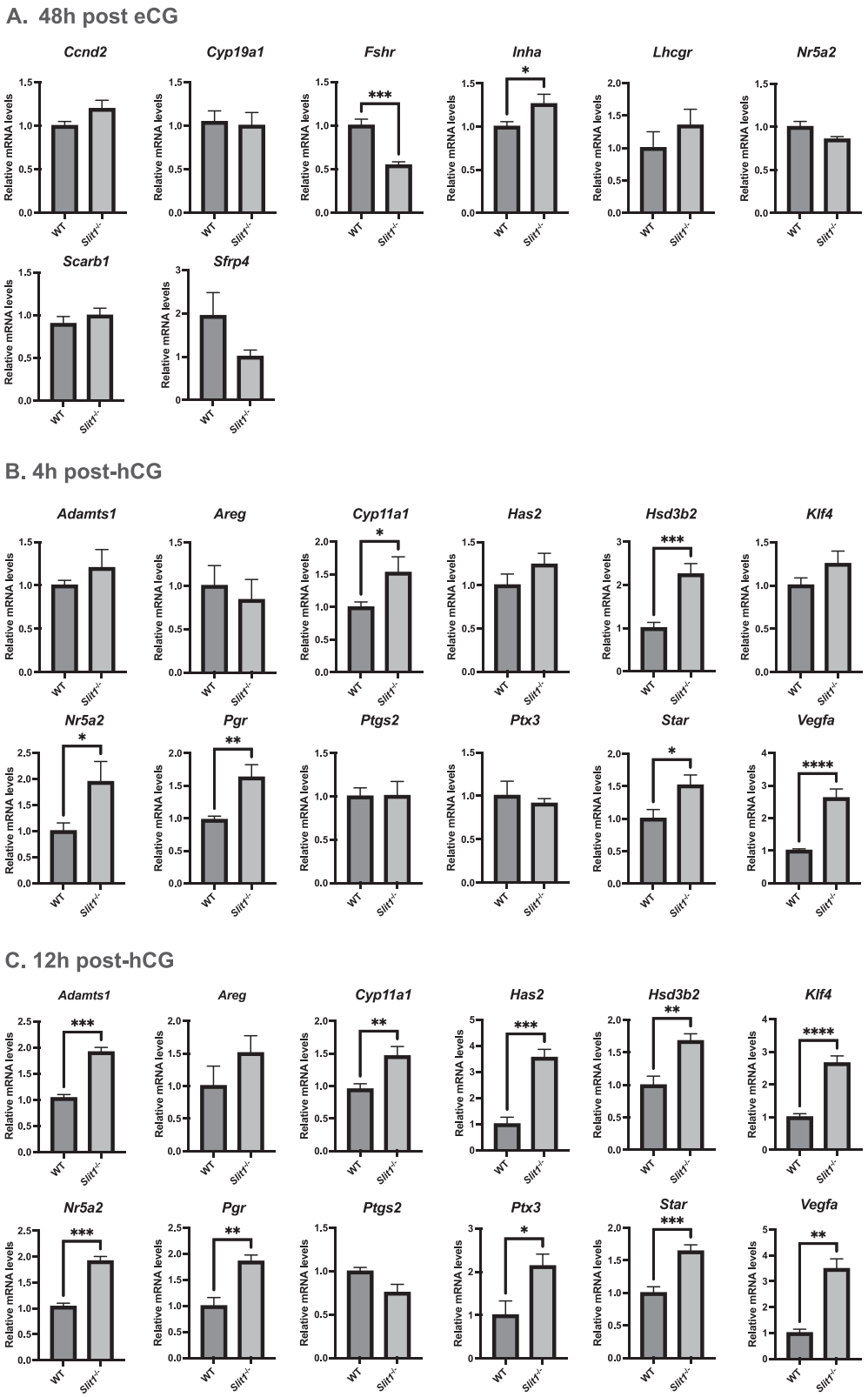

Figure 3. Alterations in gonadotropin response gene mRNA levels in the granulosa cells of *Slit1*-null mice. RT-qPCR analyses of mRNA levels of the indicated genes in granulosa cells isolated from the ovaries of immature mice 48 h following eCG treatment (A), or from eCG-primed mice 4 h (B) or 12 h (C) following an ovulatory dose of hCG ($n = 5$/group). Columns = means, error bars = SEM, statistically significant differences between groups are indicated with asterisks (*: $P < 0.05$, **: $P < 0.01$, ***: $P < 0.001$, ****: $P < 0001$).

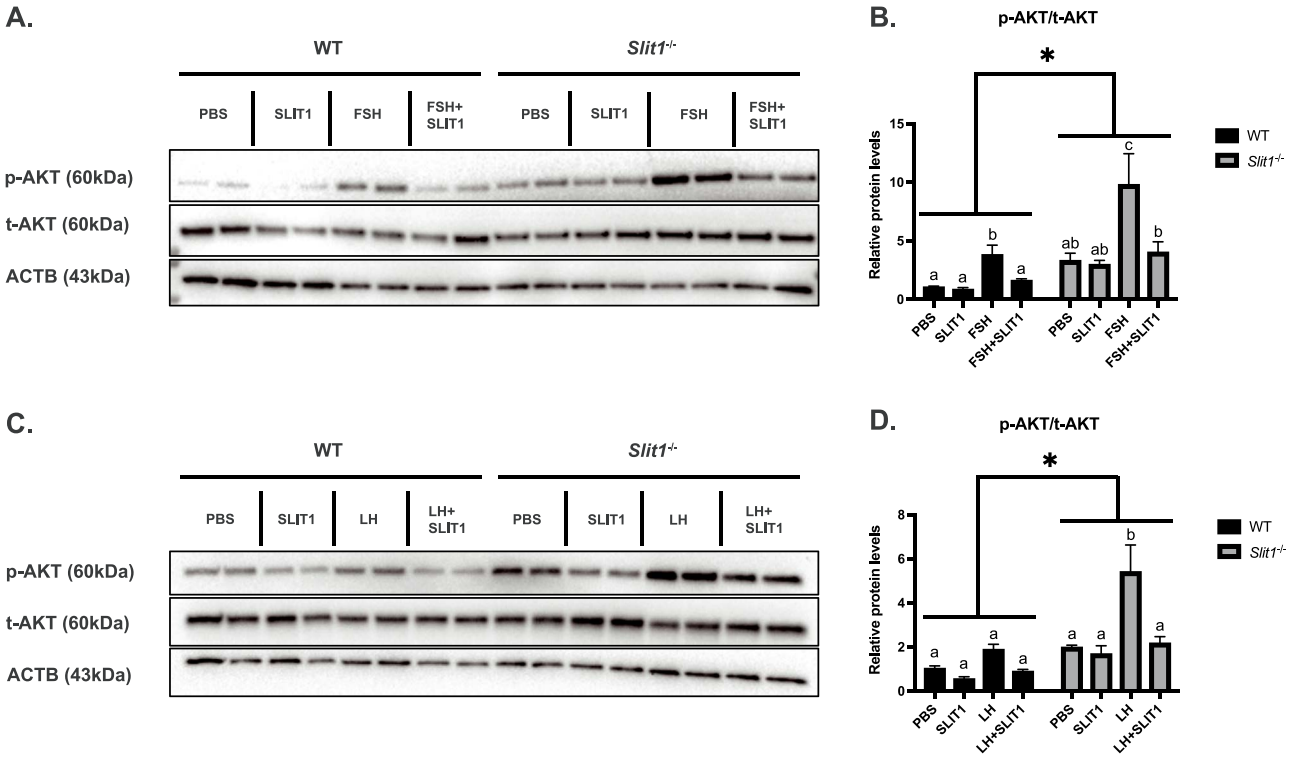

Figure 4. Increased endogenous and gonadotropin-stimulated phospho-AKT levels in the granulosa cells of Slit1-null mice. (A) Immunoblotting analyses of total AKT (t-AKT) and phospho AKT (p-AKT) levels in granulosa cells from mice of the indicated genotypes, pretreated or not with SLIT1 (10 μg/ml) prior to treatment (or not) with FSH. ACTB (β-actin) served as a loading control. (B) Densitometric analysis of the immunoblotting experiment depicted in (A) ($n = 6$/group). (C) Same as (A), except cells were treated with LH rather than FSH. (D) Densitometric analysis of the immunoblotting experiment depicted in (C) ($n = 4$/group). Columns = means, error bars = SEM, statistically significant differences between genotypes ($P < 0.05$) are indicated with an asterisk (*); columns lacking a common letter are significantly different ($P < 0.05$) from one another.

phenotype. Indeed, enhanced AKT signaling and increased mRNA levels of LH target genes involved in processes such as follicle rupture and cumulus expansion were observed in response to hCG in *Slit1*-null mice. These effects could not be attributed to increased *Lhcgr* expression and are therefore presumably the result of the loss of *Slit1*-regulated signaling processes. Although it is well established that AKT is activated by LH, its roles in mediating the biological effects of LH have not been characterized as extensively as its roles in mediating the effects of FSH. Most studies thus far suggest that LH-regulated AKT activity serves as a survival signal [52], but evidence for its involvement in LH-regulated activities such as ovulation and luteal steroidogenesis is scant. It therefore seems likely that the increase in expression in LH target genes observed in the granulosa cells of ovulatory follicles of *Slit1*-null mice involves mechanisms other than (or in addition to) enhanced AKT signaling. If suppression of AKT by *Slit1* does indeed serve to promote luteal cell apoptosis, this finding would be consistent with a previous study, which found that the addition of a chimeric ROBO1/Fc protein (which inhibits Slit/Robo signaling by sequestering SLIT ligands) to cultured human lutein cells resulted in decreased apoptosis [34]. While the latter study proposed that this could be indicative of a role for Slit/Robo signaling in mediating luteolysis, our histologic analyses of ovaries from *Slit1*-null mice showed no obvious impairment of this process. Further analyses would however be required to determine if subtle changes in apoptosis occur in luteal cells in absence of *Slit1*.

SLIT1 treatment of granulosa cells resulted in the down-regulation of *Star* mRNA levels and progesterone secretion in vitro, and granulosa cells from *Slit1*-null mice had correspondingly increased expression of *Star* and of genes involved in progesterone biosynthesis. We therefore expected to find increased serum progesterone levels in *Slit1*-null mice, but found no evidence for this in either eCG/hCG-treated immature mice or in adult mice. Progesterone production by the CL is thought to be regulated mainly at the level of the expression of *Star*, and it is not thought to be stored in meaningful amounts in luteal cells [53]. As such, it seems unlikely that the lack of increase in circulating progesterone in *Slit1*-null mice could be explained by altered release by the CL. Progesterone has a short elimination half-life (minutes) and is metabolized in large part by the liver and by the CL itself [54–56], so compensatory changes in metabolism might provide part of the answer. Further experiments would be required to test this hypothesis.

In summary, this study shows that *Slit1* represents an important new regulator of granulosa cell apoptosis and follicular atresia, and adds SLITs to the list of ovarian autocrine/paracrine signaling molecules that regulate follicle development. Future studies will be required to define the mechanisms of action of *Slit1*, including the potential genomic and nongenomic means by which it induces apoptosis, how its signal is transduced, and how it modulates gonadotropin signaling. Similarities between the ovarian phenotypes of *Slit1*-null and *Robo1/2* haploinsufficient mice [30] suggest that the former may represent the physiological ligand of the latter, though

this remains to be proven, and the physiological (and potentially redundant) roles of *Slit2* and *Slit3* in the ovary remain to be determined.

Acknowledgment

The authors thank Francis Marien-Bourgeois for technical assistance and Tristan Juette for expert advice regarding statistical methods. The graphical abstract was created using BioRender (BioRender.com).

Supplementary data

Supplementary data are available at *BIOLRE* online.

Conflict of interest: The authors have declared that no conflict of interest exists.

Author contributions

All authors participated in the study design, data analysis, and the preparation of the manuscript. FG, EM, MB, and PG performed the experiments.

Data availability

The authors confirm that the data supporting the findings of this study are available within the article and the supplementary materials.

References

1. Greenblatt RB, Mahesh VB. Pituitary-ovarian relationships. *Metabolism* 1965; **14**:320–326.
2. Hsueh AJ, Rauch R. Ovarian kaleidoscope database: ten years and Beyond1. *Biol Reprod* 2012; **86**:192.
3. Kumar TR, Wang Y, Lu N, Matzuk MM. Follicle stimulating hormone is required for ovarian follicle maturation but not male fertility. *Nat Genet* 1997; **15**:201–204.
4. Abel MH, Wootton AN, Wilkins V, Huhtaniemi I, Knight PG, Charlton HM. The effect of a null mutation in the follicle-stimulating hormone receptor gene on mouse. *Reproduction* 2000; **141**:1795–1803.
5. Fan H-Y, Liu Z, Shimada M, Sterneck E, Johnson PF, Hedrick SM, Richards JS. MAPK3/1 (ERK1/2) in ovarian granulosa cells are essential for female fertility. *Science* 2009; **324**: 938–941.
6. Zhang F-P, Poutanen M, Wilbertz J, Huhtaniemi I. Normal prenatal but arrested postnatal sexual development of luteinizing hormone receptor knockout (LuRKO). *Mice* 2001; **15**:172–183.
7. Dierich A, Sairam MR, Monaco L, Fimia GM, Gansmuller A, LeMeur M, Sassone-Corsi P. Impairing follicle-stimulating hormone (FSH) signaling in vivo: targeted disruption of the FSH receptor leads to aberrant gametogenesis and hormonal imbalance. *Proc Natl Acad Sci* 1998; **95**:13612–13617.
8. Couse JF, Korach KS. Exploring the role of sex steroids through studies of receptor deficient mice. *J Mol Med* 1998; **76**:497–511.
9. Wang H-X, Li T, Kidder GM. WNT2 regulates proliferation of mouse granulosa cells through Beta-catenin. *Biol Reprod* 2009; **81**: 376–376.
10. Wang H-X, Gillio-Meina C, Chen S, Gong X-Q, Li TY, Bai D, Kidder GM. The canonical WNT2 pathway and FSH interact to regulate gap junction assembly in mouse granulosa Cells1. *Biol Reprod* 2013; **89**:39.
11. Boyer A, Lapointe É, Zheng X, Cowan RG, Li H, Quirk SM, Demayo FJ, Richards JS, Boerboom D. WNT4 is required for normal ovarian follicle development and female fertility. *FASEB J* 2010; **24**:3010–3025.
12. Baker J, Hardy MP, Zhou J, Bondy C, Lupu F, Bellvé AR, Efstratiadis A. Effects of an Igf1 gene null mutation on mouse reproduction. *Mol Endocrinol* 1996; **10**:903–918.
13. Zhou J, Kumar TR, Matzuk MM, Bondy C. Insulin-like growth factor I regulates gonadotropin responsiveness in the murine ovary. *Mol Endocrinol* 1997; **11**:1924–1933.
14. Lapointe E, Boyer A, Rico C, Paquet M, Franco HL, Gossen J, DeMayo FJ, Richards JS, Boerboom D. FZD1 regulates cumulus expansion genes and is required for normal female fertility in Mice1. *Biol Reprod* 2012; **87**:104.
15. Norman RJ, Wu R. The potential danger of COX-2 inhibitors. *Fertil Steril* 2004; **81**:493–494.
16. Hussein TS, Froiland DA, Amato F, Thompson JG, Gilchrist RB. Oocytes prevent cumulus cell apoptosis by maintaining a morphogenic paracrine gradient of bone morphogenetic proteins. *J Cell Sci* 2005; **118**:5257–5268.
17. Sanfins A, Rodrigues P, Albertini DF. GDF-9 and BMP-15 direct the follicle symphony. *J Assist Reprod Genet* 2018; **35**:1741–1750.
18. Hayashi M, Mcgee EA, Min G, Klein C, Rose UM, Duin MV, Hsueh AJW. Recombinant growth differentiation Factor-9 (GDF-9) enhances growth and differentiation of cultured early ovarian follicles*. *Endocrinology* 1999; **140**:1236–1244.
19. Ashkenazi H, Cao X, Motola S, Popliker M, Conti M, Tsafriri A. Epidermal growth factor family members: endogenous mediators of the ovulatory response. *Endocrinology* 2005; **146**:77–84.
20. Hsieh M, Lee D, Panigone S, Horner K, Chen R, Theologis A, Lee DC, Threadgill DW, Conti M. Luteinizing hormone-dependent activation of the epidermal growth factor network is essential for ovulation. *MCB* 2007; **27**:1914–1924.
21. Gara RK, Kumari S, Ganju A, Yallapu MM, Jaggi M, Chauhan SC. Slit/Robo pathway: a promising therapeutic target for cancer. *Drug Discov Today* 2015; **20**:156–164.
22. Huang T, Kang W, Cheng ASL, Yu J, To KF. The emerging role of Slit-Robo pathway in gastric and other gastro intestinal cancers. *BMC Cancer* 2015; **15**:950.
23. Blockus H, Chédotal A. Slit-Robo signaling. *Development* 2016; **143**:3037–3044.
24. Gu F, Ma Y, Zhang J, Qin F, Fu L. Function of Slit/Robo signaling in breast cancer. *Front Med* 2015; **9**:431–436.
25. Zelina P, Blockus H, Zagar Y, Péres A, Friocourt F, Wu Z, Rama N, Fouquet C, Hohenester E, Tessier-Lavigne M, Schweitzer J, Crollius HR, *et al.* Signaling switch of the axon guidance receptor Robo3 during vertebrate evolution. *Neuron* 2014; **84**:1258–1272.
26. Zeleznik AJ, Saxena D, Little-Ihrig L. Protein kinase B is obligatory for follicle-stimulating hormone-induced granulosa cell differentiation. *Endocrinology* 2003; **144**:3985–3994.
27. Zhou P, Baumgarten SC, Wu Y, Bennett J, Winston N, Hirshfeld-Cytron J, Stocco C. IGF-I Signaling is essential for FSH stimulation of AKT and steroidogenic genes in granulosa cells. *Mol Endocrinol* 2013; **27**:511–523.
28. Fukuda S, Orisaka M, Tajima K, Hattori K, Kotsuji F. Luteinizing hormone-induced Akt phosphorylation and androgen production are modulated by MAP kinase in bovine theca cells. *J Ovarian Res* 2009; **2**:17.
29. Qin N, Fan XC, Zhang YY, Xu XX, Tyasi TL, Jing Y, Mu F, Wei ML, Xu RF. New insights into implication of the SLIT/ROBO pathway in the prehierarchical follicle development of hen ovary. *Poult Sci* 2015; **94**:2235–2246.
30. Li J, Ye Y, Zhang R, Zhang L, Hu X, Han D, Chen J, He X, Wang G, Yang X, Wang L. Robo1/2 regulate follicle atresia through manipulating granulosa cell apoptosis in mice. *Sci Rep* 2015; **5**:9720.
31. Hatzirodos N, Irving-Rodgers HF, Hummitzsch K, Harland ML, Morris SE, Rodgers RJ. Transcriptome profiling of granulosa cells of bovine ovarian follicles during growth from small to large antral sizes. *BMC Genomics* 2014; **15**:24.

32. Zhang X, Li J, Liu J, Luo H, Gou K, Cui S. Prostaglandin F2 α upregulates Slit/Robo expression in mouse corpus luteum during luteolysis. *J Endocrinol* 2013; **218**:299–310.
33. Dickinson RE, Hryhorskyj L, Tremewan H, Hogg K, Thomson AA, McNeilly AS, Duncan WC. Involvement of the SLIT/ROBO pathway in follicle development in the fetal ovary. *Reproduction* 2010; **139**:395–407.
34. Dickinson RE, Myers M, Duncan WC. Novel regulated expression of the SLIT/ROBO pathway in the ovary: possible role during Luteolysis in women. *Endocrinology* 2008; **149**:5024–5034.
35. Xu R, Qin N, Xu X, Sun X, Chen X, Zhao J. Implication of SLIT3-ROBO1/ROBO2 in granulosa cell proliferation, differentiation and follicle selection in the prehierarchical follicles of hen ovary: SLIT3 in hen ovarian prehierarchical follicle. *Cell Biol Int* 2018; **42**: 1643–1657.
36. Xu R, Qin N, Xu X, Sun X, Chen X, Zhao J. Inhibitory effect of SLIT2 on granulosa cell proliferation mediated by the CDC42-PAKs-ERK1/2 MAPK pathway in the prehierarchical follicles of the chicken ovary. *Sci Rep* 2018; **8**:9168.
37. Plump AS, Erskine L, Sabatier C, Brose K, Epstein CJ, Goodman CS, Mason CA, Tessier-Lavigne M. Slit1 and Slit2 cooperate to prevent premature midline crossing of retinal axons in the mouse visual system. *Neuron* 2002; **33**:219–232.
38. Soares MJ, Hunt JS (eds.). *Placenta and Trophoblast: Methods and Protocols Volume 1*, vol. **121**. Totowa, NJ: Humana Press; 2006.
39. Zamberlam G, Lapointe E, Abedini A, Rico C, Godin P, Paquet M, DeMayo FJ, Boerboom D. SFRP4 is a negative regulator of ovarian follicle development and female fertility. *Endocrinology* 2019; **160**: 1561–1572.
40. Pedersen T, Peters H. Proposal for a classification of oocytes and follicles IN the mouse ovary. *Reproduction* 1968; **17**:555–557.
41. Godin P, Tsoi MF, Morin M, Gévry N, Boerboom D. The granulosa cell response to luteinizing hormone is partly mediated by YAP1-dependent induction of amphiregulin. *Cell Commun Signal* 2022; **20**:72.
42. Godin P, Tsoi M, Paquet M, Boerboom D. YAP and TAZ are required for the postnatal development and the maintenance of the structural integrity of the oviduct. *Reproduction* 2020; **160**: 307–318.
43. Pfaffl MW. A new mathematical model for relative quantification in real-time RT-PCR. *Nucleic Acids Res* 2001; **29**:45e–445e.
44. Schneider CA, Rasband WS, Eliceiri KW. NIH image to ImageJ: 25 years of image analysis. *Nat Methods* 2012; **9**:671–675.
45. Maidana DE, Tsoka P, Tian B, Dib B, Matsumoto H, Kataoka K, Lin H, Miller JW, Vavvas DG. A novel ImageJ macro for automated cell death quantitation in the retina. *Invest Ophthalmol Vis Sci* 2015; **56**:6701–6708.
46. Zhang X, Mi M, Hao W, Fan Q, Gao B. Progesterone down-regulates SLIT/ROBO expression in mouse corpus luteum. *Acta Histochem* 2017; **119**:740–746.
47. Pinho AV, Van Bulck M, Chantrill L, Arshi M, Sklyarova T, Herrmann D, Vennin C, Gallego-Ortega D, Mawson A, Giry-Laterriere M, Magenau A, Leuckx G, *et al.* ROBO2 is a stroma suppressor gene in the pancreas and acts via TGF-β signalling. *Nat Commun* 2018; **9**:5083.
48. Tseng R-C, Lee S-H, Hsu H-S, Chen B-H, Tsai W-C, Tzao C, Wang Y-C. SLIT2 attenuation during lung cancer progression deregulates β-catenin and E-cadherin and associates with poor prognosis. *Cancer Res* 2010; **70**:543–551.
49. Conti M, Hsieh M, Musa Zamah A, Oh JS. Novel signaling mechanisms in the ovary during oocyte maturation and ovulation. *Mol Cell Endocrinol* 2012; **356**:65–73.
50. Carvalho CRO, Carvalheira JBC, Lima MHM, Zimmerman SF, Caperuto LC, Amanso A, Gasparetti AL, Meneghetti V, Zimmerman LF, Velloso LA, Saad MJA. Novel signal transduction pathway for luteinizing hormone and its interaction with insulin: activation of Janus kinase/signal transducer and activator of transcription and Phosphoinositol 3-kinase/Akt pathways. *Endocrinology* 2003; **144**:638–647.
51. Kumariya S, Ubba V, Jha RK, Gayen JR. Autophagy in ovary and polycystic ovary syndrome: role, dispute and future perspective. *Autophagy* 2021; **17**:2706–2733.
52. Herndon MK, Law NC, Donaubauer EM, Kyriss B, Hunzicker-Dunn M. Forkhead box O member FOXO1 regulates the majority of follicle-stimulating hormone responsive genes in ovarian granulosa cells. *Mol Cell Endocrinol* 2016; **434**:116–126.
53. Casarini L, Santi D, Brigante G, Simoni M. Two hormones for one receptor: evolution, biochemistry, actions, and pathophysiology of LH and hCG. *Endocr Rev* 2018; **39**:549–592.
54. Niswender GD, Juengel JL, Silva PJ, Rollyson MK, McIntush EW. Mechanisms controlling the function and life span of the corpus luteum. *Physiol Rev* 2000; **80**:1–29.
55. Mesen TB, Young SL. Progesterone and the luteal phase. *Obstet Gynecol Clin North Am* 2015; **42**:135–151.
56. Coombes Z, Plant K, Freire C, Basit AW, Butler P, Conlan RS, Gonzalez D. Progesterone metabolism by human and rat hepatic and intestinal tissue. *Pharmaceutics* 2021; **13**:1707.